# Current Concepts in $^{68}$Ga-DOTATATE Imaging of Neuroendocrine Neoplasms: Interpretation, Biodistribution, Dosimetry, and Molecular Strategies

Lisa Bodei[1], Valentina Ambrosini[2], Ken Herrmann[3,4], and Irvin Modlin[5]

*[1]Molecular Imaging and Therapy Service, Department of Radiology, Memorial Sloan Kettering Cancer Center, New York, New York; [2]Nuclear Medicine, Department of Experimental Diagnostic and Specialized Medicine, University of Bologna and S. Orsola-Malpighi Hospital, Bologna, Italy; [3]Department of Molecular and Medical Pharmacology, David Geffen School of Medicine at UCLA, Los Angeles, California; [4]Klinik für Nuklearmedizin, Universitätsklinikum Essen, Essen, Germany; and [5]Yale University School of Medicine, Department of Surgery, New Haven, Connecticut*

**Learning Objectives:** On successful completion of this activity, participants should be able to describe (1) the role of $^{68}$Ga-DOTATATE in neuroendocrine tumor management, (2) the interpretation of $^{68}$Ga-DOTATATE PET/CT images, and (3) the integration of $^{68}$Ga-DOTATATE PET/CT in the diagnostic and management algorithm for neuroendocrine tumors.

**Financial Disclosure:** Dr. Bodei is a consultant/advisor for Ipsen and AAA Pharmaceutical, and Dr. Herrmann is a consultant/advisor for Ipsen, Curium, and Sofie Biosciences and an investigator for AAA Pharmaceutical. The authors of this article have indicated no other relevant relationships that could be perceived as a real or apparent conflict of interest.

**CME Credit:** SNMMI is accredited by the Accreditation Council for Continuing Medical Education (ACCME) to sponsor continuing education for physicians. SNMMI designates each *JNM* continuing education article for a maximum of 2.0 AMA PRA category 1 credits. Physicians should claim only credit commensurate with the extent of their participation in the activity. For CE credit, SAM, and other credit types, participants can access this activity through the SNMMI website (http://www.snmmilearningcenter.org) through November 2020.

$^{68}$Ga-DOTATATE PET/CT provides information on the location of somatostatin receptor–expressing tumors. Integrating this imaging data effectively in patient care requires the clinical history; the histopathology and biomarker information; and the grade, stage, and prior imaging results. Previous therapies and technical aspects of the study should be considered, given their ability to alter the interpretation of the images. This includes physiologic biodistribution of the radiotracer, as well as conditions that engender false-positive results. This article provides a guide to the performance and interpretation of $^{68}$Ga-DOTATATE PET/CT and describes its role in the diagnostic algorithm of neuroendocrine neoplasms and its overall utility in their management.

**Key Words:** endocrine; neuroendocrine; oncology; peptides; $^{68}$Ga-DOTATATE; biodistribution

**J Nucl Med 2017; 58:1718–1726**
DOI: 10.2967/jnumed.116.186361

Neuroendocrine neoplasms exhibit variable symptomatology, such as tumor mass effects or the biologic consequences of the bioactive amine secretion, frequently delaying diagnosis. Some patients present with symptoms related to inappropriate peptide or amine hypersecretion, but most of these tumors are nonfunctioning. Nonfunctioning tumors are usually discovered when they are large and have metastasized to the liver. Thus, even though the lesions are mostly well differentiated and slow-growing, with a minority of aggressive forms, the outcome may be poor because of diagnostic delay (*1*).

Somatostatin receptor (SSR) imaging offers an opportunity to identify receptor-expressing neuroendocrine neoplasms (NENs) (*2,3*). Radiolabeled somatostatin analogs (SSA) were introduced in the 1980s for imaging of NENs (Fig. 1) (*4,5*).

## CLINICAL SCENARIO

NENs are relatively rare tumors originating from ubiquitous neuroendocrine cells distributed throughout the body. These cells synthesize, store, and secrete various circulating hormones and neurotransmitters (Table 1) (*6*).

NENs constitute 0.66% of all malignancies in the United States, according to the Surveillance, Epidemiology, and End Results database, containing 48,195 NENs from 1970 to 2006, with an incidence increasing at a rate of 3%–10% per year (*7*). This increment is related to the introduction of more sensitive diagnostic tools and to an increased awareness by clinicians and pathologists (*1,8*). The prevalence of NENs is substantial given the often indolent nature of the disease process. Most (66%) arise in the gastroenteropancreatic area, and 25% occur in the lung (*7*). The recognition that the prevalence of NENs as a gastrointestinal cancer is exceeded only by that of colon cancer has increased focus on the problem (*1*).

Less frequent forms of NENs include pheochromocytoma, paraganglioma, medullary thyroid carcinoma, and neuroblastoma. Pheochromocytoma and paragangliomas derive from sympathetic chromaffin tissue in the adrenal medulla and from the extraadrenal paraganglial system of the thorax and abdomen (*9*). The frequent malignant propensity of these tumors reflects the genetic background. More than 50% of tumors are due to genetic

Received May 8, 2017; revision accepted Jul. 27, 2017.
For correspondence or reprints contact: Lisa Bodei, Molecular Imaging and Therapy Service, Department of Radiology, Memorial Sloan Kettering Cancer Center, 1275 York Ave., Box 77, New York, NY 10065.
E-mail: bodeil@mskcc.org
Published online Aug. 17, 2017.

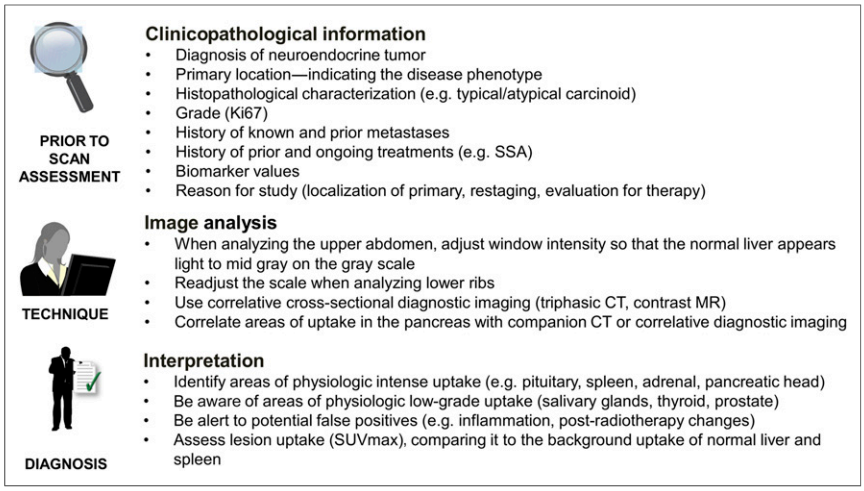


**FIGURE 1.** Optimal strategy for $^{68}$Ga-DOTATATE PET/CT evaluation.

alterations (*10*). Pheochromocytoma exhibits an overall incidence of 0.8 cases/100,000/y over 30 y in the white population, according to the Rochester Epidemiology Project (*11*).

## CLASSIFICATION

Since 1963, many NEN classifications have been adopted, based on the embryologic origin of the tumor (foregut, midgut, hindgut), degree of differentiation, and site of origin (*12*). The term *carcinoid* has been abandoned for gastroenteropancreatic NENs. The prognostic assessment of gastroenteropancreatic NENs has improved significantly since the introduction of the European Neuroendocrine Tumor Society and World Health Organization 2010 staging and grading systems. The World Health Organization 2010 classification scores gastroenteropancreatic NENs as G1, G2, or G3 on the basis of the morphology and Ki-67 scoring index (gastroenteropancreatic neuroendocrine tumor G1, Ki-67 $<$ 2%; neuroendocrine tumor G2, Ki-67 = 3%–20%; neuroendocrine carcinoma G3, Ki-67 $>$ 20%) and mixed adenoneuroendocrine carcinoma (*13*). Although most NENs are well differentiated (G1 or G2), around 5.6%–8% are G3 (Ki-67 $>$ 20%) (*14*). Recent evidence highlights the need to further stratify patients in the G3 group as well-differentiated neuroendocrine tumor G3 (Ki-67 = 20%–50%) or poorly differentiated neuroendocrine carcinoma G3 (Ki-67 $>$ 50%) on the basis of their different clinical behavior and response to treatment.

The current classification of bronchopulmonary NENs includes typical and atypical carcinoid, large cell neuroendocrine carcinoma, small cell carcinoma, and (considered a preinvasive form) diffuse idiopathic pulmonary neuroendocrine cell hyperplasia. A new classification of lung neuroendocrine tumors has been proposed by the World Health Organization (*15*) and was endorsed by the European Neuroendocrine Tumor Society. Like the system for gastroenteropancreatic NENs, this 3-tier grading system is centered on the Ki-67 index, with specifically generated cutoffs (bronchopulmonary NEN G1, Ki-67 $<$ 4%, no necrosis; G2, Ki-67 = 4%–25% and necrosis in fewer than 10 high-power fields; G3, Ki-67 $>$ 25% and necrosis in more than 10 high-power fields).

**TABLE 1**
Gastrointestinal and Pancreatic Neuroendocrine Cell Types and Secretory Products

| Cell type | Localization | Products |
|---|---|---|
| Delta | Entire gastrointestinal tract | Somatostatin |
| Enterochromaffin | Entire gastrointestinal tract | Serotonin/substance P/guanylin/melatonin |
| Enterochromaffinlike | Gastric fundus | Histamine |
| Gastrin | Gastric antrum and duodenum | Gastrin |
| Ghrelin | Entire gastrointestinal tract | Ghrelin |
| I | Duodenum | Cholecystokinin |
| K | Duodenum/jejunum | Gastric inhibitory peptide |
| L | Small intestine | GLP-1, PYY, NPY |
| Motilin | Duodenum | Motilin |
| Neurotensin | Small intestine | Neurotensin |
| Secretin | Duodenum | Secretin |
| Vasoactive intestinal peptide | Entire gastrointestinal tract | Vasoactive intestinal peptide |
| X | Gastric fundus and antrum | Amylin |
| Beta | Pancreas | Insulin |
| Alpha | Pancreas | Glucagon |
| Delta | Pancreas | Somatostatin |
| Pancreatic polypeptide | Pancreas | Pancreatic polypeptide |

GLP-1 = glucagonlike peptide 1; PYY = polypeptide YY (tyrosine, tyrosine); NPY = neuropeptide Y (tyrosine).

The tumor grade, histopathology type, primary site, and stage reflect the potential metastatic spread and, therefore, the impact on tumor burden and the subsequent choice of therapeutic options (Table 2). Knowledge of these characteristics, together with the prior treatment history, is fundamental in the interpretation of a $^{68}$Ga-DOTATATE image.

## $^{68}$GA-DOTATATE PET/CT

### Indications

$^{68}$Ga-DOTATATE is a radiolabeled SSA indicated for use with PET or PET/CT for localization of SSR-positive NENs in adult and pediatric patients (*16*).

SSR imaging is used for staging and restaging and to select patients for peptide receptor radionuclide therapy (PRRT) with cold or radiolabeled SSAs (*17,18*). The rationale for SSR imaging is the tumor cell receptor–mediated internalization of the receptor-radio-analog complex and its retention in the cytoplasm.

### Three SSA Peptides and Choice of DOTATATE

$^{111}$In-pentetreotide, or OctreoScan (Mallinckrodt), was the first approved radiopharmaceutical for NEN imaging. Over the past 15 y, this tracer demonstrated the utility of SSR imaging. The development of $^{68}$Ga-labeled agents suitable for use with PET/CT has markedly enhanced lesion detection (because of improved resolution) and quantitation with the $^{68}$Ga-labeled octreotide derivatives ($^{68}$Ga-SSA PET/CT) DOTATOC, DOTANOC, and DOTATATE (*18–20*). These analogs retain an octreotidelike affinity profile and, in particular, high affinity for somatostatin receptor 2 (e.g., 0.2 ± 0.04 nM for somatostatin receptor 2 with $^{68}$Ga-DOTATATE, much greater than the 22 ± 3.6 nM with $^{111}$In-pentetreotide (*21*)). Only $^{68}$Ga-DOTANOC exhibits substantial affinity for somatostatin receptor 3 (*22*). Despite these differences in receptor affinity, a clear superiority of one compound over the others has not been demonstrated. A comparison of $^{68}$Ga-DOTATOC versus $^{68}$Ga-DOTATATE PET/CT in the same patients yielded comparable diagnostic accuracy, despite potential advantages for $^{68}$Ga-DOTATOC in the higher number of detected lesions and the higher $SUV_{max}$ (*23*). However, a recent comparison of $^{68}$Ga-DOTATATE and $^{68}$Ga-DOTANOC PET/CT in the same NEN patients showed a higher $SUV_{max}$ for $^{68}$Ga-DOTATATE on a lesion basis and comparable diagnostic accuracy on a patient basis (*24*). The inconclusive results on this issue reported in the literature possibly reflect the particular receptor configuration of the individual tumors and the lack of internationally recognized criteria for SSR PET interpretation.

On the basis of the demonstrated superiority of $^{68}$Ga-DOTATATE PET/CT imaging compared with $^{111}$In-octreotide, the U.S. Food and Drug Administration has approved $^{68}$Ga-DOTATATE for localization of SSR-positive neuroendocrine tumors in adult and pediatric patients.

### Technique

The potential benefits of withdrawal of SSA treatment, or at least of scanning patients at the end of the coverage period of the analog, is still under debate, and no international consensus has been reached. If discontinuation is clinically feasible and performed, short-acting analogs should be stopped for at least 48 h and long-acting formulations for 4–6 wk (*16*). Recent data investigating the impact of SSA on $^{68}$Ga-DOTATATE PET/CT in the same patients studied on and off treatment on 2 consecutive days do not support the need for discontinuation. The authors reported reduced uptake at physiologic sites with unchanged tumor uptake in the patients under treatment, resulting in higher image contrast (*25*). Since normal organ and tumor uptake tends to increase the later the PET scan occurs after SSA administration (*26*), and since rigorous data on timing are unavailable, many centers scan patients at the end of the SSA treatment cycle, if possible (e.g., before the subsequent SSA injection), otherwise maintaining the same interval from the SSA injection as in the previous scan.

According to the recent European Association of Nuclear Medicine guidelines and the U.S. Food and Drug Administration–approved label, the recommended activity to obtain good image quality is 2 MBq/kg of body weight (0.054 mCi/kg) up to 200 MBq (5.4 mCi), administered as an intravenous bolus injection.

$^{68}$Ga-DOTATATE can be supplied either already labeled or as a kit to be reconstituted according to the manufacturer's (Advanced Accelerator Applications) instructions (http://www.accessdata.fda.gov/drugsatfda_docs/label/2016/208547s000lbl.pdf).

Before injection, the radioactivity should be verified with a dose calibrator. Injected radioactivity should be within ±10% of the recommended dose.

Patients should be encouraged to drink a sufficient amount of water before tracer administration (e.g., 1 L, if tolerated, with or without oral contrast medium) and after tracer administration to increase image quality in the abdomen, and to void frequently.

The PET/CT acquisition typically begins 45–60 min after the intravenous administration of the radiopeptide and proceeds from the top of the skull to the mid thighs, preferably in a 3-dimensional mode. A detailed description of the scanning protocol and image reconstruction is provided in the European Association of Nuclear Medicine procedure guidelines for $^{68}$Ga-DOTA-peptides (*16,27*). The use of intravenous contrast medium may further enhance detection. However, in standard use, unenhanced PET/CT is considered sufficient.

### Biodistribution

Clearance of $^{68}$Ga-DOTATATE from the blood is rapid. Dynamic PET studies demonstrated that arterial activity shows biexponential elimination, with no radioactive metabolites detected in serum or urine in the first 4 h. Radioactivity in the blood decreases to less than 5.3% of the peak level within 45 min of the dynamic scanning and to 2.2% at 195 min after injection. After 50 min, the accumulation in all organs plateaus, and maximal tumor activity accumulation is reached at 70 ± 20 min after injection (*28*). Excretion occurs almost exclusively via the kidneys.

Physiologic uptake is high in somatostatin receptor 2–rich organs such as the pituitary gland, spleen, adrenals, liver, pelvicalyceal system of the kidneys, and urinary bladder. Lower uptake may physiologically be observed in the thyroid, pancreatic head, stomach, small and large bowel, and prostate (Fig. 2) (*29*).

SUV has been demonstrated to correlate with receptor density up to values of approximately 25, corresponding to the steady-state inhibition constant value of 0.2 mL/cm$^3$/min, after which the relationship is not linear. This may lead to underestimation of receptor expression (*28*).

### Dosimetry

Estimated absorbed doses per injected activity for organs and tissues follow the biodistribution, peaking at 1, 2, and 3 h after injection in the spleen, followed by kidneys, and liver (Table 3). The highest absorbed doses are observed in the spleen and urinary bladder wall, followed by the kidneys, adrenals, and liver. The reported total effective dose was 0.021 ± 0.003 mSv/MBq (*30*).

**TABLE 2**
Site and Clinical Presentation of Gastroenteropancreatic and Bronchopulmonary NENs

| Site | Clinical presentation |
|---|---|
| Gastrointestinal | |
| Gastric | Type I: atrophic gastritis, gastrin-dependent |
| | Type II (MEN1): menin-dependent, gastrin-related (Zollinger-Ellison syndrome) |
| | Type III: gastrin-independent, clinically aggressive |
| Duodenal | Various phenotypes: gastrinoma, so-called carcinoid, somatostatinoma |
| Jejunal | "Carcinoid": classic symptoms (flushing, diarrhea), clinically aggressive |
| Ileal | "Carcinoid": classic symptoms (flushing, diarrhea), clinically aggressive; typical CT appearance of contrast-enhancing spiculated mass, sometimes containing calcifications, surrounded by lines of desmoplastic reactions |
| Appendiceal | "Carcinoid": usually present as appendicitis or incidental finding at laparotomy/laparoscopy and generally radically cured after surgical excision |
| | Goblet cell "carcinoid" (mucinous carcinoid): clinically aggressive |
| Colonic | Carcinoid symptoms are rare, and presentation is similar to adenocarcinoma |
| Rectal | Local manifestations: pain, bleeding |
| Hepatic | >95% are metastases from gastroenteropancreatic NEN primary; typical CT appearance of hypodense masses, with rich enhancement during arterial phase, reverting to hypodense during portal phase; on MRI (most sensitive technique), lesions enhance after gadolinium, and best sequences are arterial phase and fast spin-echo T2-weighted |
| Pancreatic | |
| Gastrinoma (Zollinger-Ellison syndrome) | Peptic ulceration and secretory diarrhea; 60%–90% malignant behavior |
| Insulinoma | Hypoglycemia, generally small and SSR-negative; 5%–15% malignant and generally SSR-positive |
| Glucagonoma | Skin rash (migrating necrolytic erythema), weight loss, diabetes; 60% malignant |
| VIPoma | Secretory diarrhea (Verner–Morrison syndrome); 80% malignant |
| Somatostatinoma | Diabetes, gallstones, often component of genetic syndrome; 60% malignant |
| GRFoma | Acromegaly; 30% malignant |
| ACTHoma | Cushing syndrome; aggressive behavior; >90% malignant |
| P-NEN causing carcinoid syndrome | Diarrhea, flushing; 68%–88% malignant |
| P-NEN causing hypercalcemia | Hypercalcemia; 80%–90% malignant |
| Nonfunctioning | Local mass effects; 60%–90% malignant |
| Bronchopulmonary | |
| Typical carcinoid | Frequently central, with cough, wheezing, hemoptysis, and signs of bronchial obstruction; functional when metastatic (carcinoid, Cushing, acromegaly, or syndrome of inappropriate antidiuretic hormone secretion); relatively indolent biologic behavior; may be part of MEN1 |
| Atypical carcinoid | Frequently peripheral and asymptomatic, may present with coughing and wheezing or functional syndrome; from indolent to aggressive; may be part of MEN1 |
| Large cell neuroendocrine carcinoma | Aggressively metastatic and rapidly progressing |
| Small cell lung cancer | Aggressively metastatic and rapidly progressing |
| Thymic neuroendocrine tumors | Frequently large, 50% functional, usually adrenocorticotropic hormone–induced Cushing syndrome; frequently metastatic; may be part of MEN1 |
| Chromaffin | |
| Pheochromocytoma/paraganglioma | 80%–85% arise from adrenal medulla, 15%–20% extraadrenal; majority associated with catecholamine hypersecretion (most frequently, hypertension, tachycardia, headache, pallor, sweating, and anxiety), with frequent paroxysmal component |

VIP = vasoactive intestinal peptide; GRF = growth hormone–releasing factor; ACTH = adrenocorticotropic hormone; P-NEN = pancreatic neuroendocrine neoplasm.

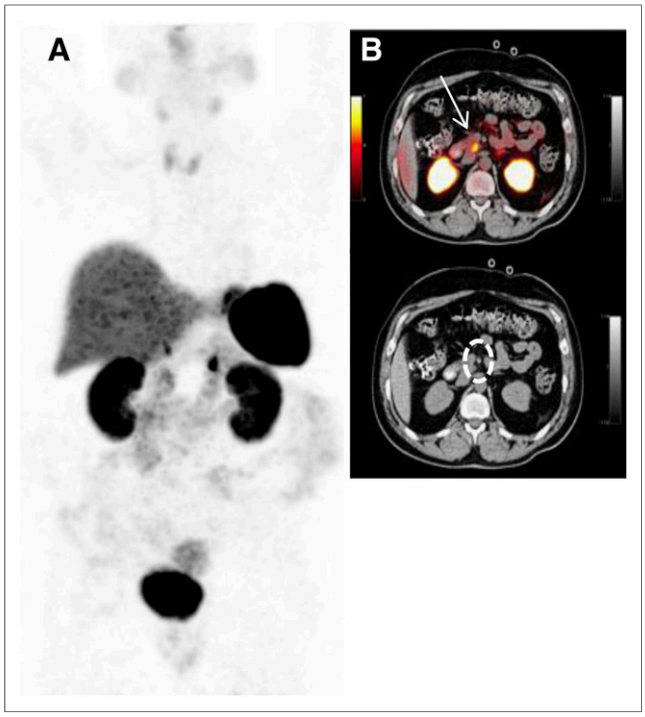


**FIGURE 2.** (A) Normal biodistribution of $^{68}$Ga-DOTATATE on volumetric (maximum-intensity-projection, MIP) image. (B) Axial PET/CT images showing physiologic intense uptake in pituitary, liver, spleen, kidneys, adrenals, and uncinate process of pancreas (arrow and oval outline) and variable degree of uptake in thyroid, intestine, and urinary bladder.

The effective radiation dose resulting from the administration of 185 MBq (5 mCi) to an adult weighing 75 kg is about 4.8 mSv (*31*). For this activity, the typical radiation dose to the critical organs, which are the urinary bladder wall, the spleen, and the kidneys, are about 0.125, 0.282, and 0.0921 mSv/MBq, respectively (*31*). Since the spleen has the highest physiologic uptake, higher uptake and dose to normal or tumor tissues may occur in patients with splenectomy, as demonstrated for $^{68}$Ga-DOTATOC (*32*). The effective dose deriving from the low-dose CT component is generally in the range of 9 mSv for 80-mA low-dose CT, whereas for 10-mA ultra-low-dose CT it is closer to 1 mSv.

### Interpretation

Assessment of images should be guided by clinical information. As a general rule, besides areas of physiologic uptake, clearly outlined foci of uptake should be regarded as positive for SSR expression and thus considered to potentially represent NEN (Fig. 3 and Supplemental Fig. 1; supplemental materials are available at http://jnm.snmjournals.org). $^{68}$Ga-DOTATATE has certain limitations that have to be considered in order to adequately interpret the corresponding scans. There are alternative conditions that may exhibit increased SSR expression and, hence, represent potential sources of false-positives (Figs. 4 and 5 and Supplemental Fig. 2). These mainly include areas of inflammation or infection containing activated lymphocytes and macrophages, such as radiation pneumonitis, gastritis, sequelae of recent surgeries, reactive lymphadenopathy, and granulomatous lesions. For example, the thyroid generally exhibits low-grade uptake ($SUV_{max}$ of 1.4–7.7, $SUV_{mean}$ of 3.0 (*29*)). More intense diffuse uptake could represent thyroiditis (due to the SSR-positive diffuse lymphocyte infiltration), whereas focal uptake could represent nodular disease (*33*). An area that requires careful consideration is the head of the pancreas, particularly the uncinate process, which may exhibit a variable physiologic uptake—focal or diffuse—of $^{68}$Ga-DOTATATE, related to the great concentration of pancreatic polypeptide cells (*16*). This represents a potential source of misinterpretation, since the pancreas and the duodenum are frequent sites of NENs. There have been attempts at defining an $SUV_{max}$ threshold to distinguish benign from malignant pancreatic uptake of DOTA-SSA peptides (*34,35*). However, given the large overlap between benign/physiologic and malignant uptake and the large interscanner measurement variance, mere uptake should not be used to diagnose pancreatic NENs without the demonstration of a clear lesion on the companion CT image or at correlative diagnostic cross-sectional imaging (*36*). Other common non–NEN-related sources of uptake include accessory spleens or splenules, which could be erroneously interpreted as lymph nodes. If accessory spleens are sufficiently large, consideration of lesion attenuation and arterial-phase contrast behavior may be of assistance (Fig. 6).

Prolonged therapy with cold SSA may reduce the background physiologic uptake to the spleen and liver.

False-negatives are most commonly related to lesion size (spatial resolution is around 5.5–7 mm, with potential additional detrimental effects due to partial-volume effect, Fig. 7), recent analog therapy (although this issue is debated), alteration of receptor expression by recent chemotherapy, or truly receptor-negative disease (e.g., benign insulinomas and high-grade NENs). In the case of high-grade tumors, correlation with $^{18}$F-FDG PET/CT may be useful. High physiologic uptake as previously described in organs such as the spleen, liver, adrenals, pituitary gland; in the pelvicalyceal system of the kidneys and urinary bladder; and to a lesser degree in the thyroid, pancreatic head, stomach, small and large bowel, and prostate can mask isointense or slight pathologic somatostatin receptor 2 expression.

### Clinical Value

$^{68}$Ga-DOTA-peptide PET/CT is the gold standard functional imaging modality to study well-differentiated NENs in Europe and is included in European guidelines (*16*). Over the past decade, many reports have demonstrated the superiority of SSR PET/CT (with $^{68}$Ga-DOTATATE, $^{68}$Ga-DOTATOC, or $^{68}$Ga-DOTANOC)

**TABLE 3**
Absorbed Doses of $^{68}$Ga-DOTATATE in Selected Organs

| Site | Absorbed dose (mGy/MBq ± SD) | |
|---|---|---|
| | Sandström et al. (*30*) | Walker et al. (*31*) |
| Kidney | 0.093 ± 0.016 | 0.092 ± 0.028 |
| Liver | 0.050 ± 0.015 | 0.045 ± 0.015 |
| Gallbladder wall | 0.016 ± 0.002 | 0.015 ± 0.001 |
| Spleen | 0.109 ± 0.058 | 0.028 ± 0.121 |
| Adrenals | 0.086 ± 0.052 | 0.015 ± 0.001 |
| Lungs | 0.006 ± 0.001 | 0.012 ± 0.0004 |
| Urinary bladder wall | 0.098 ± 0.048 | 0.125 ± 0.062 |
| Red marrow | 0.015 ± 0.003 | 0.010 ± 0.0004 |
| Total body | 0.014 ± 0.002 | 0.013 ± 0.0003 |
| Effective dose (mSv/MBq) | 0.021 ± 0.003 | 0.026 ± 0.003 |

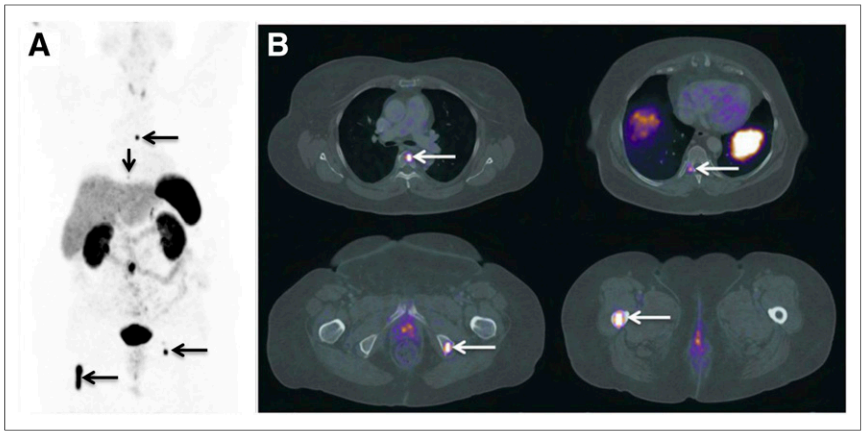


**FIGURE 3.** Upstaging of patient with history of small intestine NEN and 6.5-cm lesion within right proximal femur with benign appearance at prior MRI. (A) DOTATATE maximum-intensity-projection image revealed multiple mesenteric and pelvic, as well as multiple unexpected osseous, metastases (arrows). (B) On axial PET/CT, the unexpected soft-tissue and bone metastases were detected in more detail (arrows). Intended treatment was converted from surgery and octreotide to surgery, octreotide, and selective radiotherapy of bone metastases. (Adapted from (*66*).)

over single-photon scintigraphy (including SPECT/CT), morphologic imaging (CT/MRI), or PET/CT with other radiopharmaceuticals (*16,19,20,37–41*). In a recent prospective trial including 131 patients with gastroenteropancreatic NENs and unknown primary NENs, $^{68}$Ga-DOTATATE showed a higher detection rate (95.2%) than $^{111}$In-pentetreotide SPECT/CT (30.9%) or CT or MRI (45.6%) (*42*).

The largest single study specifically addressing $^{68}$Ga-DOTATATE diagnostic accuracy in NENs (*39*) was retrospective and included 728 patients and 1,258 PET/CT scans. $^{68}$Ga-DOTATATE PET/CT showed high sensitivity (>94%) and specificity (>92%) for NEN lesion localization, with the highest accuracy being for primary midgut tumors. The results of that study are in line with those of much smaller previous studies using PET/CT with either $^{68}$Ga-DOTATOC or $^{68}$Ga-DOTANOC (*16,20,43–46*). Overall, SSR PET/CT showed a high accuracy (≥96%) for the detection of well-differentiated NENs at either the primary site or the metastatic sites (mostly lymph nodes, liver, bone, and lung) (*20,39,44*).

Current guidelines indicate the high diagnostic accuracy of SSR PET/CT for detection of disease extension (at both staging and restaging), identification of the unknown primary site, and selection of candidates for PRRT (*16*).

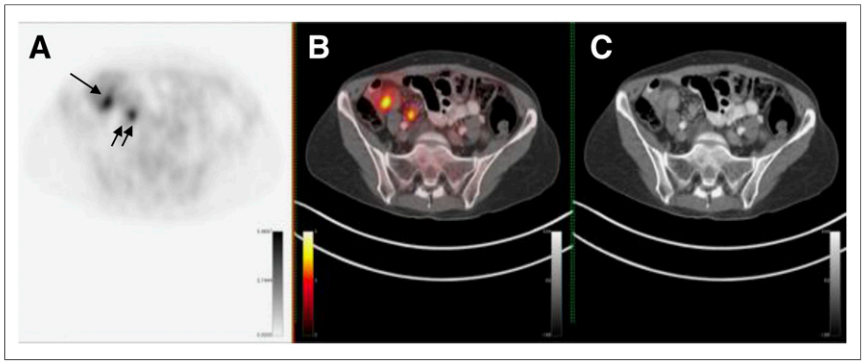


**FIGURE 4.** Patient with ileal neuroendocrine tumor (single arrow) who showed additional focal $^{68}$Ga-DOTATATE uptake (doubled arrow) in pelvis on imaging. Shown are axial PET (A), PET/CT (B), and CT (C) images. PET/CT images clarified this finding as physiologic uptake in right ureter.

The role of PET/CT for the assessment of tumor response to treatment is still under debate since a reduction of uptake can indicate a reduction of tumor volume (and of receptor number) but cannot exclude the presence of undifferentiated clones that may be SSR-negative. Considering the fact that SSR PET/CT positivity predicts the localization of cold and radiolabeled SSA-based treatment options, it is evident that the clinical impact of $^{68}$Ga-DOTATATE lies not merely in better diagnostic accuracy but also in better therapeutic management with cold SSA or PRRT.

A recently published systematic review (*47*) (including data from 1,561 patients) reported an overall change in management in 44% (range, 16%–71%) after $^{68}$Ga-SSA PET/CT (with either $^{68}$Ga-DOTATOC, $^{68}$Ga-DOTATATE, or $^{68}$Ga-DOTANOC). About half of these cases were provided by a single study using $^{68}$Ga-DOTATATE (728/1,561, or 47%) (*39*). In that study, Skoura et al. found that the treatment plan was changed in 40.9% (515/1,278) of the $^{68}$Ga-DOTATATE PET/CT cases because of new, unexpected findings. In most cases, the new treatment comprised chemotherapy or PRRT (362/515, or 70.3%), whereas less frequent options included surgery (after detection or confirmation of the NEN primary site, 52/515, or 10.1%) and second-line chemotherapy (71/515, or 13.8%). Less common management changes included ongoing-treatment discontinuation (2/515), rejection of PRRT (2/515), and selection of liver transplant candidates by excluding extrahepatic disease (2/515). Previous reports on smaller patient populations reported similar findings (*42*).

$^{68}$Ga-SSA PET/CT has also been demonstrated to provide relevant prognostic information: since the intensity of uptake is an indirect measure of tumor differentiation, higher uptake correlated with a better prognosis (*48*).

The role of $^{68}$Ga-SSA PET/CT in G3 NENs is debated. By definition, G3 includes poorly differentiated tumors. However, especially in the subgroup with a Ki-67 of 20%–50%, the clinical behavior is more similar to G2 tumors. In this setting, a complementary role with $^{18}$F-FDG can therefore be envisioned. Vice versa, $^{68}$Ga-SSA PET/CT in cases presenting higher Ki-67 values (>50%), even if positive, will likely not affect management.

The added value of $^{18}$F-FDG in well-differentiated NENs (G1 and G2) is still under debate, and no international consensus has been reached (*49–53*).

According to current evidence, it is not routinely recommended that $^{18}$F-FDG should have a role in G1 NENs (a role in which its use could be considered only in selected cases when a specific clinical indication or suspicion is present), whereas $^{18}$F-FDG may have a clinical role in G2 NENs, especially for higher Ki-67 values, based on clinical indications (e.g., patients with CT progression or with SSR PET/CT-negative lesions). Recently, it was in fact

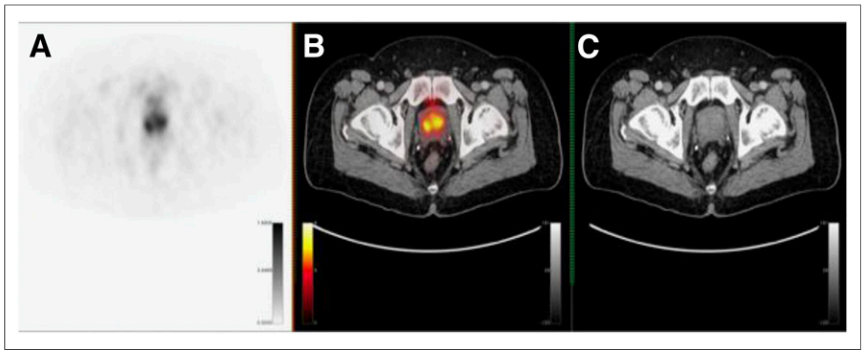


**FIGURE 5.** Increased $^{68}$Ga-DOTATATE prostatic uptake. Shown are axial PET (A), PET/CT (B), and CT (C) images. Patient had known benign prostatic hyperplasia, and corresponding uptake is therefore non–tumor-specific.

shown that $^{18}$F-FDG PET/CT should be used only in selected cases, with a Ki-67 of less than 12% (*53*), as in such cases the clinical management uniquely relies on $^{68}$Ga-DOTATATE.

Current European Neuroendocrine Tumor Society guidelines (*54*) indicate a potential role for $^{18}$F-FDG only for the G3 group, when surgery is indicated. Several studies, mostly retrospective, investigated the role of combination of $^{68}$Ga-SSA PET/CT and $^{18}$F-FDG PET/CT in NENs. However, they were hampered by a small patient population and by the heterogeneity of the tumor primary site (a well-known factor affecting $^{18}$F-FDG positivity). In a recent multinational, multidisciplinary Delphi consensus meeting of NEN experts ($n = 33$) (*55*), $^{18}$F-FDG PET/CT was considered valuable for differentiating high- from low-grade tumors and for its prognostic implications. No consensus, however, was reached regarding combining $^{18}$F-FDG and $^{68}$Ga-SSA PET/CT or their timing in a diagnostic setting.

A combined imaging modality to achieve a complete biologic characterization defining a more aggressive behavior is appealing. In fact, the mere detection of a higher number of lesions or even the detection of $^{18}$F-FDG positivity is not necessarily associated with a different management in all cases or in all nuclear medicine or oncology departments. However, there is international consensus on the fact that $^{18}$F-FDG positivity correlates with a worse prognosis (*56*), but the treatment strategies to be implemented in $^{18}$F-FDG–positive cases are not standardized. The rationale for using $^{18}$F-FDG relies on its ability to identify the presence of aggressive disease foci—an ability that may turn into a better stratification of patients at major risk of progression. The clinical scenario of double-tracer imaging findings ranges from purely SSR-positive/$^{18}$F-FDG–negative cases to $^{18}$F-FDG–positive/SSR-negative cases, with a very heterogeneous intermediate group presenting various patterns of uptake in the same patient with both tracers in the same or in different lesions over time (*52*). The most important lesson deriving from these studies is the demonstration of the heterogeneous nature of NENs.

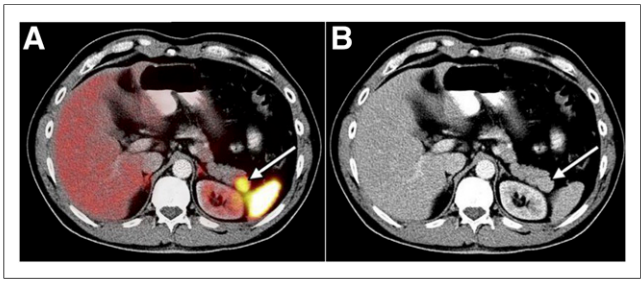


**FIGURE 6.** Patient with repeated flushing who underwent $^{68}$Ga-DOTATATE PET/CT. Shown are axial PET/CT (A) and CT (B) images. Focal uptake (arrow) in pancreatic tail was characterized on the basis of clinical data and MRI, indicating presence of splenule abutting tail of pancreas. (Reprinted from (*47*).).

SSR imaging is used to select patients for PRRT. Although the criteria are well defined and validated for $^{111}$In-pentetreotide with the 4-point Krenning scale, which is based on relative tumor uptake compared with uptake by normal organs (liver, kidneys, and spleen, where grade 1 is uptake less than liver [liver excluded], grade 2 is uptake equal to liver, grade 3 is uptake greater than liver, and grade 4 is uptake much greater than kidneys and spleen) (*4*), there is no consensus on what should be considered sufficient uptake at $^{68}$Ga-SSA PET/CT. Some authors have reported $SUV_{max}$ thresholds for PRRT enrollment based on retrospective analyses (e.g., an $SUV_{max}$ of 17.9 (*57*) or 16.4 (*58*) for $^{68}$Ga-DOTATOC). However, this approach is hampered by the limited reproducibility of $SUV_{max}$ across different scanners. More frequently in clinical practice, the Krenning scale is adapted to the volumetric $^{68}$Ga-SSA PET/CT image, and lesion uptake greater than liver is considered suitable for PRRT.

### Integration Within the Diagnostic Algorithm of NENs

Biomarkers are a viable adjunct to image interpretation. The secretory activity of NENs is quantifiable and facilitates their detection. Previously, chromogranin A was considered useful, but rigorous assessment over the last decade has led to decreased enthusiasm about its use, because of normal levels in about 30%–40% of NENs and falsely elevated levels in patients with renal failure, cardiac disease, or proton pump inhibitor therapy (*59*). Moreover, alterations in circulating chromogranin A levels are often nonconcordant with imaging, and prospective studies have not confirmed a role for chromogranin A in predicting or defining progression (*55*). To better reflect not only the mere secretory activity but also the complex biologic activities of an evolving neoplasm (cell proliferation, growth factor signaling, and others) that constitute the hallmarks of cancer, and to provide more relevant information on tumor behavior, new approaches have been introduced, including whole-genome sequencing, circulating micro-RNA, and tumor transcripts (*60*). Evaluation of circulating messenger RNA (transcript analysis) has provided information on disease status that is of substantial clinical utility in the management of NENs (*61,62*). This strategy uses simultaneous polymerase chain reaction–based analyses of multiple neuroendocrine tumor genes measurable in the blood and algorhythmic transformation into a mathematic index of disease activity (*60,63*). NEN gene blood levels correlated with $^{68}$Ga-DOTA-SSA PET/CT imaging and could define disease status (*64*).

Current imaging strategies and biomarkers in NEN management addressed at a recent Delphi consensus meeting of NEN experts (*55*) indicated agreement on the use of CT or MRI in conjunction with functional imaging. Because of its synergistic value, $^{68}$Ga-DOTATATE is often used in addition to morphologic imaging modalities such as CT and MRI. PET/CT scanners are widely available, and the corresponding CT, if performed with diagnostic quality and contrast medium, may improve the diagnostic accuracy, particularly in

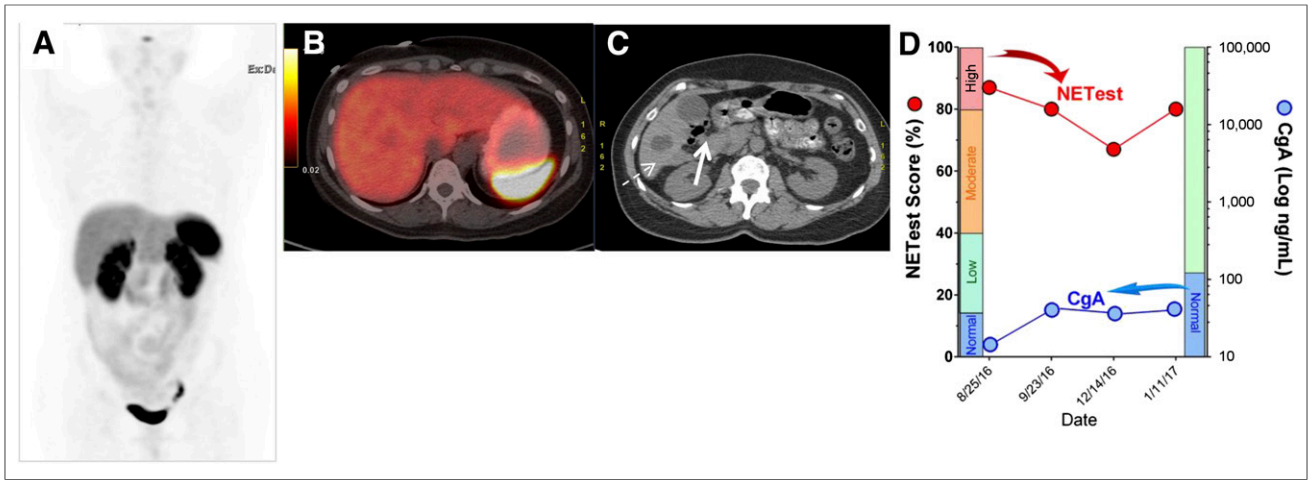


**FIGURE 7.** 60-y-old woman who had previously undergone ileal neuroendocrine tumor resection, was currently on SSA with associated cholelithiasis, and was scheduled for surgery. Before surgery, $^{68}$Ga-DOTATATE PET/CT (volumetric image [A] and axial [B]) and chromogranin A (D, blue circles) were negative. However, circulating neuroendocrine transcript levels (red circles) were positive. Positive transcript levels indicate presence of primary, residual, or metastatic neuroendocrine tumor. At cholecystectomy, there was no evidence of hepatic metastases. Random intraoperative hepatic needle biopsy, however, demonstrated presence of neuroendocrine tumor metastases. (C) Axial CT scan showing cholelithiasis (solid arrow) and simple hepatic cyst (dashed arrow).

organs with high physiologic $^{68}$Ga-DOTATATE uptake and in the lungs. Especially, gastroenteropancreatic NENs are well suited for dedicated PET/MRI, as MRI adds important information to the detection of abdominal lesions, particularly in the liver (Supplemental Fig. 3) (*65,66*), whereas CT remains superior for the detection and characterization of lung lesions. As discussed, $^{18}$F-FDG detects dedifferentiated lesions expressing no or little somatostatin receptor 2 (*54*). A common indication for $^{18}$F-FDG PET/CT is morphologically growing lesions with a discordant $^{68}$Ga-DOTATATE finding.

These observations are worthy of further clinical study to provide evidence that the interface of imaging and circulating molecular indices of tumor evolution is likely to enhance dynamic assessment of tumor status.

## CONCLUSION

$^{68}$Ga-DOTA-peptide PET/CT has significantly advanced the approach to NENs. Its widespread implementation is based on its proven clinical utility and facilitation of clinical management. Overall, it represents the gold standard functional imaging modality for the assessment of well-differentiated NENs in conjunction with anatomic imaging (CT or MRI). An unmet need is the evaluation of the clinical impact of the dual-approach $^{18}$F-FDG and $^{68}$Ga-SSA PET/CT in the decision-making algorithm, given the numerous indications from the literature of the prognostic impact of $^{18}$F-FDG avidity in terms of overall and treatment-specific survival. A further significant advance needed is the development of an accurate, personalized interpretation of the individual disease status. This personalization may be accomplished by an algorithmic integration of the clinical, histopathologic, imaging, and molecular information available for the neoplasm of each subject.

## REFERENCES


1. Modlin IM, Oberg K, Chung DC, et al. Gastroenteropancreatic neuroendocrine tumours. *Lancet Oncol.* 2008;9:61–72.
2. Sundin A. Radiological and nuclear medicine imaging of gastroenteropancreatic neuroendocrine tumours. *Best Pract Res Clin Gastroenterol.* 2012;26:803–818.
3. Oberg K. Diagnostic work-up of gastroenteropancreatic neuroendocrine tumors. *Clinics (Sao Paulo).* 2012;67(suppl 1):109–112.
4. Kwekkeboom DJ, Kam BL, van Essen M, et al. Somatostatin-receptor-based imaging and therapy of gastroenteropancreatic neuroendocrine tumors. *Endocr Relat Cancer.* 2010;17:R53–R73.
5. Crona J, Skogseid B. GEP- NETS UPDATE: genetics of neuroendocrine tumors. *Eur J Endocrinol.* 2016;174:R275–R290.
6. Polak JM, Bloom SR. Regulatory peptides of the gastrointestinal and respiratory tracts. *Arch Int Pharmacodyn Ther.* 1986;280:16–49.
7. Gustafsson BI, Kidd M, Modlin IM. Neuroendocrine tumors of the diffuse neuroendocrine system. *Curr Opin Oncol.* 2008;20:1–12.
8. Modlin IM, Champaneria MC, Chan AK, Kidd M. A three-decade analysis of 3,911 small intestinal neuroendocrine tumors: the rapid pace of no progress. *Am J Gastroenterol.* 2007;102:1464–1473.
9. Tumours of the adrenal gland: WHO and TNM classifications. In: DeLellis RA, Lloyd RV, Heitz PU, Eng C, eds. *Pathology and Genetics: Tumours of the Endocrine Organs.* Lyon, France: IARC Press; 2004.
10. Favier J, Amar L, Gimenez-Roqueplo AP. Paraganglioma and phaeochromocytoma: from genetics to personalized medicine. *Nat Rev Endocrinol.* 2015;11:101–111.
11. Beard CM, Sheps SG, Kurland LT, Carney JA, Lie JT. Occurrence of pheochromocytoma in Rochester, Minnesota, 1950 through 1979. *Mayo Clin Proc.* 1983;58:802–804.
12. Williams ED, Sandler M. The classification of carcinoid tumours. *Lancet.* 1963;1:238–239.
13. Rindi G, Arnold R, Bosman FT. Nomenclature and classification of neuroendocrine neoplasms of the digestive system. In: Bosman FT, Carneiro F, Hruban RH, Theise ND, eds. *WHO Classification of Tumours of the Digestive System.* Lyon, France: IARC Press; 2010.
14. Vélayoudom-Céphise FL, Duvillard P, Foucan L, et al. Are G3 ENETS neuroendocrine neoplasms heterogeneous? *Endocr Relat Cancer.* 2013;20:649–657.
15. Travis WD, Brambilla E, Nicholson AG, et al. The 2015 World Health Organization Classification of lung tumors: impact of genetic, clinical and radiologic advances since the 2004 classification. *J Thorac Oncol.* 2015;10:1243–1260.
16. Virgolini I, Ambrosini V, Bomanji JB, et al. Procedure guidelines for PET/CT tumour imaging with $^{68}$Ga-DOTA-conjugated peptides: $^{68}$Ga-DOTA-TOC, $^{68}$Ga-DOTA-NOC, $^{68}$Ga-DOTA-TATE. *Eur J Nucl Med Mol Imaging.* 2010;37:2004–2010.
17. Bodei L, Sundin A, Kidd M, Prasad V, Modlin IM. The status of neuroendocrine tumor imaging: from darkness to light? *Neuroendocrinology.* 2015;101:1–17.
18. Ambrosini V, Morigi JJ, Nanni C, Castellucci P, Fanti S. Current status of PET imaging of neuroendocrine tumours ([$^{18}$F]FDOPA, [$^{68}$Ga]tracers, [$^{11}$C]/[$^{18}$F]-HTP). *Q J Nucl Med Mol Imaging.* 2015;59:58–69.
19. Treglia G, Castaldi P, Rindi G, Giordano A, Rufini V. Diagnostic performance of gallium-68 somatostatin receptor PET and PET/CT in patients with thoracic and gastroenteropancreatic neuroendocrine tumours: a meta-analysis. *Endocrine.* 2012;42:80–87.

20. Gabriel M, Decristoforo C, Kendler D, et al. $^{68}$Ga-DOTA-Tyr3-octreotide PET in neuroendocrine tumors: comparison with somatostatin receptor scintigraphy and CT. *J Nucl Med.* 2007;48:508–518.
21. Reubi JC, Schar JC, Waser B, et al. Affinity profiles for human somatostatin receptor subtypes SST1-SST5 of somatostatin radiotracers selected for scintigraphic and radiotherapeutic use. *Eur J Nucl Med.* 2000;27:273–282.
22. Reubi JC, Waser B, Schaer JC, Laissue JA. Somatostatin receptor sst1-sst5 expression in normal and neoplastic human tissues using receptor autoradiography with subtype-selective ligands. *Eur J Nucl Med.* 2001;28:836–846.
23. Poeppel TD, Binse I, Petersenn S, et al. $^{68}$Ga-DOTATOC versus $^{68}$Ga-DOTATATE PET/CT in functional imaging of neuroendocrine tumors. *J Nucl Med.* 2011; 52:1864–1870.
24. Kabasakal L, Demirci E, Ocak M, et al. Comparison of $^{68}$Ga-DOTATATE and $^{68}$Ga-DOTANOC PET/CT imaging in the same patient group with neuroendocrine tumours. *Eur J Nucl Med Mol Imaging.* 2012;39:1271–1277.
25. Interim results on the influence of lanreotide on uptake of [$^{68}$Ga]-DOTATATE in patients with metastatic or unresectable NET: no evidence for discontinuation of lanreotide before [$^{68}$Ga]-DOTATATE PET/CT. *Clin Adv Hematol Oncol.* 2016;14:13–15.
26. Haug AR, Rominger A, Mustafa M, et al. Treatment with octreotide does not reduce tumor uptake of $^{68}$Ga-DOTATATE as measured by PET/CT in patients with neuroendocrine tumors. *J Nucl Med.* 2011;52:1679–1683.
27. Bozkurt MF, Virgolini I, Balogova S, et al. Guideline for PET/CT imaging of neuroendocrine neoplasms with $^{68}$Ga-DOTA-conjugated somatostatin receptor targeting peptides and $^{18}$F-DOPA. *Eur J Nucl Med Mol Imaging.* 2017;44:1588–1601.
28. Velikyan I, Sundin A, Sorensen J, et al. Quantitative and qualitative intrapatient comparison of $^{68}$Ga-DOTATOC and $^{68}$Ga-DOTATATE: net uptake rate for accurate quantification. *J Nucl Med.* 2014;55:204–210.
29. Shastry M, Kayani I, Wild D, et al. Distribution pattern of $^{68}$Ga-DOTATATE in disease-free patients. *Nucl Med Commun.* 2010;31:1025–1032.
30. Sandström M, Velikyan I, Garske-Roman U, et al. Comparative biodistribution and radiation dosimetry of $^{68}$Ga-DOTATOC and $^{68}$Ga-DOTATATE in patients with neuroendocrine tumors. *J Nucl Med.* 2013;54:1755–1759.
31. Walker RC, Smith GT, Liu E, Moore B, Clanton J, Stabin M. Measured human dosimetry of $^{68}$Ga-DOTATATE. *J Nucl Med.* 2013;54:855–860.
32. Kratochwil C, Mavriopoulou E, Rath D, et al. Comparison of $^{68}$Ga-DOTATOC biodistribution in patients with and without spleenectomy. *Q J Nucl Med Mol Imaging.* 2015;59:116–120.
33. Lincke T, Singer J, Kluge R, Sabri O, Paschke R. Relative quantification of indium-111 pentetreotide and gallium-68 DOTATOC uptake in the thyroid gland and association with thyroid pathologies. *Thyroid.* 2009;19:381–389.
34. Prasad V, Baum RP. Biodistribution of the Ga-68 labeled somatostatin analogue DOTA-NOC in patients with neuroendocrine tumors: characterization of uptake in normal organs and tumor lesions. *Q J Nucl Med Mol Imaging.* 2010;54:61–67.
35. Kroiss A, Putzer D, Decristoforo C, et al. $^{68}$Ga-DOTA-TOC uptake in neuroendocrine tumour and healthy tissue: differentiation of physiological uptake and pathological processes in PET/CT. *Eur J Nucl Med Mol Imaging.* 2013;40:514–523.
36. Virgolini I, Gabriel M, Kroiss A, et al. Current knowledge on the sensitivity of the $^{68}$Ga-somatostatin receptor positron emission tomography and the SUVmax reference range for management of pancreatic neuroendocrine tumours. *Eur J Nucl Med Mol Imaging.* 2016;43:2072–2083.
37. Ambrosini V, Tomassetti P, Castellucci P, et al. Comparison between $^{68}$Ga-DOTA-NOC and $^{18}$F-DOPA PET for the detection of gastro-entero-pancreatic and lung neuro-endocrine tumours. *Eur J Nucl Med Mol Imaging.* 2008;35:1431–1438.
38. Srirajaskanthan R, Kayani I, Quigley AM, Soh J, Caplin ME, Bomanji J. The role of $^{68}$Ga-DOTATATE PET in patients with neuroendocrine tumors and negative or equivocal findings on $^{111}$In-DTPA-octreotide scintigraphy. *J Nucl Med.* 2010;51:875–882.
39. Skoura E, Michopoulou S, Mohmaduvesh M, et al. The impact of $^{68}$Ga-DOTATATE PET/CT imaging on management of patients with neuroendocrine tumors: experience from a national referral center in the United Kingdom. *J Nucl Med.* 2016;57:34–40.
40. Deppen SA, Blume J, Bobbey AJ, et al. $^{68}$Ga-DOTATATE compared with $^{111}$In-DTPA-octreotide and conventional imaging for pulmonary and gastroenteropancreatic neuroendocrine tumors: a systematic review and meta-analysis. *J Nucl Med.* 2016;57:872–878.
41. Ambrosini V, Campana D, Tomassetti P, Fanti S. $^{68}$Ga-labelled peptides for diagnosis of gastroenteropancreatic NET. *Eur J Nucl Med Mol Imaging.* 2012;39(suppl 1):S52–S60.
42. Sadowski SM, Neychev V, Millo C, et al. Prospective study of $^{68}$Ga-DOTATATE positron emission tomography/computed tomography for detecting gastro-entero-pancreatic neuroendocrine tumors and unknown primary sites. *J Clin Oncol.* 2016;34:588–596.
43. Putzer D, Gabriel M, Henninger B, et al. Bone metastases in patients with neuroendocrine tumor: $^{68}$Ga-DOTA-Tyr3-octreotide PET in comparison to CT and bone scintigraphy. *J Nucl Med.* 2009;50:1214–1221.
44. Ambrosini V, Nanni C, Zompatori M, et al. $^{68}$Ga-DOTA-NOC PET/CT in comparison with CT for the detection of bone metastasis in patients with neuroendocrine tumours. *Eur J Nucl Med Mol Imaging.* 2010;37:722–727.
45. Haug A, Auernhammer CJ, Wangler B, et al. Intraindividual comparison of $^{68}$Ga-DOTA-TATE and $^{18}$F-DOPA PET in patients with well-differentiated metastatic neuroendocrine tumours. *Eur J Nucl Med Mol Imaging.* 2009;36:765–770.
46. Kayani I, Conry BG, Groves AM, et al. A comparison of $^{68}$Ga-DOTATATE and $^{18}$F-FDG PET/CT in pulmonary neuroendocrine tumors. *J Nucl Med.* 2009;50:1927–1932.
47. Fendler WP, Barrio M, Spick C, et al. $^{68}$Ga-DOTATATE PET/CT interobserver agreement for neuroendocrine tumor assessment: results of a prospective study on 50 patients. *J Nucl Med.* 2017;58:307–311.
48. Campana D, Ambrosini V, Pezzilli R, et al. Standardized uptake values of $^{68}$Ga-DOTANOC PET: a promising prognostic tool in neuroendocrine tumors. *J Nucl Med.* 2010;51:353–359.
49. Partelli S, Rinzivillo M, Maurizi A, et al. The role of combined Ga-DOTANOC and $^{18}$FDG PET/CT in the management of patients with pancreatic neuroendocrine tumors. *Neuroendocrinology.* 2014;100:293–299.
50. Kundu P, Lata S, Sharma P, Singh H, Malhotra A, Bal C. Prospective evaluation of $^{68}$Ga-DOTANOC PET-CT in differentiated thyroid cancer patients with raised thyroglobulin and negative $^{131}$I-whole body scan: comparison with $^{18}$F-FDG PET-CT. *Eur J Nucl Med Mol Imaging.* 2014;41:1354–1362.
51. Bahri H, Laurence L, Edeline J, et al. High prognostic value of $^{18}$F-FDG PET for metastatic gastroenteropancreatic neuroendocrine tumors: a long-term evaluation. *J Nucl Med.* 2014;55:1786–1790.
52. Nilica B, Waitz D, Stevanovic V, et al. Direct comparison of $^{68}$Ga-DOTA-TOC and $^{18}$F-FDG PET/CT in the follow-up of patients with neuroendocrine tumour treated with the first full peptide receptor radionuclide therapy cycle. *Eur J Nucl Med Mol Imaging.* 2016;43:1585–1592.
53. Panagiotidis E, Alshammari A, Michopoulou S, et al. Comparison of the impact of $^{68}$Ga-DOTATATE and $^{18}$F-FDG PET/CT on clinical management in patients with neuroendocrine tumors. *J Nucl Med.* 2017;58:91–96.
54. Garcia-Carbonero R, Sorbye H, Baudin E, et al.; Vienna Consensus Conference participants. ENETS consensus guidelines for high-grade gastroenteropancreatic neuroendocrine tumors and neuroendocrine carcinomas. *Neuroendocrinology.* 2016;103:186–194.
55. Oberg K, Krenning E, Sundin A, et al. A Delphic consensus assessment: imaging and biomarkers in gastroenteropancreatic neuroendocrine tumor disease management. *Endocr Connect.* 2016;5:174–187.
56. Binderup T, Knigge U, Loft A, Federspiel B, Kjaer A. $^{18}$F-fluorodeoxyglucose positron emission tomography predicts survival of patients with neuroendocrine tumors. *Clin Cancer Res.* 2010;16:978–985.
57. Öksuz MÖ, Winter L, Pfannenberg C, et al. Peptide receptor radionuclide therapy of neuroendocrine tumors with $^{90}$Y-DOTATOC: is treatment response predictable by pre-therapeutic uptake of $^{68}$Ga-DOTATOC? *Diagn Interv Imaging.* 2014;95:289–300.
58. Kratochwil C, Stefanova M, Mavriopoulou E, et al. SUV of [$^{68}$Ga]DOTATOC-PET/CT predicts response probability of PRRT in neuroendocrine tumors. *Mol Imaging Biol.* 2015;17:313–318.
59. Jensen EH, Kvols L, McLoughlin JM, et al. Biomarkers predict outcomes following cytoreductive surgery for hepatic metastases from functional carcinoid tumors. *Ann Surg Oncol.* 2007;14:780–785.
60. Oberg K, Modlin IM, De Herder W, et al. Consensus on biomarkers for neuroendocrine tumour disease. *Lancet Oncol.* 2015;16:e435–e446.
61. Pavel M, Jann H, Prasad V, Drozdov I, Modlin IM, Kidd M. NET blood transcript analysis defines the crossing of the clinical Rubicon: when stable disease becomes progressive. *Neuroendocrinology.* 2017;104:170–182.
62. Modlin IM, Drozdov I, Kidd M. The identification of gut neuroendocrine tumor disease by multiple synchronous transcript analysis in blood. *PLoS One.* 2013;8:e63364.
63. Modlin IM, Drozdov I, Alaimo D, et al. A multianalyte PCR blood test outperforms single analyte ELISAs (chromogranin A, pancreastatin, neurokinin A) for neuroendocrine tumor detection. *Endocr Relat Cancer.* 2014;21:615–628.
64. Bodei L, Kidd M, Modlin IM, et al. Gene transcript analysis blood values correlate with $^{68}$Ga-DOTA-somatostatin analog (SSA) PET/CT imaging in neuroendocrine tumors and can define disease status. *Eur J Nucl Med Mol Imaging.* 2015;42:1341–1352.
65. Hope TA, Pampaloni MH, Nakakura E, et al. Simultaneous $^{68}$Ga-DOTA-TOC PET/MRI with gadoxetate disodium in patients with neuroendocrine tumor. *Abdom Imaging.* 2015;40:1432–1440.
66. Beiderwellen KJ, Poeppel TD, Hartung-Knemeyer V, et al. Simultaneous $^{68}$Ga-DOTATOC PET/MRI in patients with gastroenteropancreatic neuroendocrine tumors: initial results. *Invest Radiol.* 2013;48:273–279.
67. Herrmann K, Czernin J, Wolin EM, et al. Impact of $^{68}$Ga-DOTATATE PET/CT on the management of neuroendocrine tumors: the referring physician's perspective. *J Nucl Med.* 2015;56:70–75.